Available online at www.sciencedirect.com
SCIENCE DIRECT
Journal of Magnetic Resonance 179 (2006) 294–298
JMR Journal of Magnetic Resonance
www.elsevier.com/locate/jmr

Communication

Radiation damping in microcoil NMR probes

V.V. Krishnan *

Biosciences Directorate, Lawrence Livermore National Laboratory, Livermore, CA 94551, USA

Received 27 July 2005; revised 15 December 2005
Available online 20 January 2006

Abstract

Radiation damping arises from the field induced in the receiver coil by large bulk magnetization and tends to selectively drive this magnetization back to equilibrium much faster than relaxation processes. The demand for increased sensitivity in mass-limited samples has led to the development of microcoil NMR probes that are capable of obtaining high quality NMR spectra with small sample volumes (nL–μL). Microcoil probes are optimized to increase sensitivity by increasing either the sample-to-coil ratio (filling factor) of the probe or quality factor of the detection coil. Though radiation damping effects have been studied in standard NMR probes, these effects have not been measured in the microcoil probes. Here a systematic evaluation of radiation damping effects in a microcoil NMR probe is presented and the results are compared with similar measurements in conventional large volume samples. These results show that radiation-damping effects in microcoil probe is much more pronounced than in 5 mm probes, and that it is critically important to optimize NMR experiments to minimize these effects. As microcoil probes provide better control of the bulk magnetization, with good RF and B_0 inhomogeneity, in addition to negligible dipolar field effects due to nearly spherical sample volumes, these probes can be used exclusively to study the complex behavior of radiation damping.

Keywords: Radiation damping; Microcoil probe; NMR; Water

1. Introduction

Detection of water resonances through a tuned circuit introduces an effect commonly known as radiation damping, which is a combined manifestation of the spin system and the electronic resonance circuit assembly. This phenomenon was first experimentally observed by Suryan [1], while Bloembergen and Pound [2] provided the complete mechanistic details. Qualitatively, the precessing transverse magnetization of the nuclear spins after a radio frequency pulse induces an electromagnetic field (emf) in the receiver coil (Lenz law). This induced field exerts a torque that rotates the water magnetization toward the z-axis in a tuned coil, thus giving rise to the phenomenon of radiation damping. As a result of the ~110 M concentration of water protons and of the typically high Q-factor of modern NMR probes, radiation damping occurs on a time scale of tens of milliseconds and it often interferes with solvent suppression schemes [3–5]. With the advent of ultrahigh-field magnets (900 MHz and above) and the design of supersensitive probes, the time constant for radiation damping is expected to be even shorter, thus radiation damping is one of the important problems in current NMR spectroscopy.

In general, NMR spectroscopy demands large sample volume (500–800 μL), as it is an inherently insensitive method. However, over the last decade the availability of high field super-conducting magnets (>14 T) and steady improvement in NMR probe technology have notably improved the sensitivity of detection [6]. In particular, two kinds of probe technology have been developed recently; (a) probes with cryogenically cooled detector coils [7] that have 2–4 times better sensitivity than standard probes and (b) small volume probes [8,9] that are capable of acquiring good quality NMR spectra from microliter [9]

* Current address: Department of Applied Science, University of California Davis, Davis, CA 95616, USA.
E-mail address: vvkrish@gmail.com.

1090-7807/$ - see front matter © 2006 Elsevier Inc. All rights reserved.
doi:10.1016/j.jmr.2005.12.011

down to picoliter [10] sample volumes. While cryogenically cooled probes lower the temperature to increase the sensitivity, small volume probes achieve the same by decreasing the diameter of the NMR detector coil.

Traditionally, small-volume NMR probes have found application almost exclusively in the structural analysis of mass-limited samples [11,12]. However, this trend has been changing recently as reports describing the use of such probes to study proteins [13–16] and DNA [17] have appeared. NMR studies of biological molecules require the sample to be dissolved in aqueous solutions, in particular at high percentage of H_2O. Though radiation damping effects have been studied extensively in standard probes [18–20], to my knowledge this is the first experimental work to investigate these effects in a microcoil probe. Intuitively, microcoil probes are expected to have noticeable radiation damping effects, as these probes are optimized for increased sensitivity. At the same time, the sample volume in these probes is 1–2 orders of magnitude less than the standard probes, suggesting these effects may be minimal. To understand these differences, a systematic evaluation of the effect of radiation damping in a microcoil probe, and comparison of the results with those from a similar evaluation of this effect in standard NMR probes. The results presented demonstrate that radiation damping in microcoil probes is significant and comparable to the standard 5 mm probes. These results hence suggest that precautions must be considered to suppress and eliminate these effects for optimal experimental results.

2. Materials and methods

2.1. Spectrometer and probes

All NMR experiments were performed on a Varian *INOVA* ($\nu_H = 600$ MHz) NMR spectrometer at room temperature (25 °C). Three different NMR probes were used: (a) Triple resonance capillary microcoil NMR probe (CapNMR, MRM, Savoy, USA), (b) 5 mm inverse detection (ID) probe with *Z*-gradient (Varian, Palo Alto, California, purchase year 1997, Signal-to-noise ~900:1 in standard sample), and (c) 8 mm triple-resonance, *Z*-axis gradient probe (Varian, Palo Alto, California, purchase year 1997, Signal-to-noise ~1400:1 in standard sample). Water used in the experiments was passed through a MilliQ reverse osmosis system (Milli-RX12, Nihon Millipore, Yonezawa, Japan) and a 0.05 μm polycarbonate membrane (Coster Scientific, MA). As an internal lock, D_2O (99.9% enriched, Cambridge, MA) (5% of total volume) was added.

For the CapNMR probe, the flow cell volume was 25 μL with an active volume of 5 μL. Gastight syringes (Hamilton, USA) were used to inject the water sample. The probe has an S/N ratio of 32:1 (200 Hz noise window) using a 10 mM sucrose (anomeric proton) sample in D_2O (four scans, no presaturation, and no line broadening). The total volume of the water in the 5 and 8 mm sample tubes was 550 and 730 μL, respectively. The samples were tuned using the standard Varian spectrometer's tune bridge and the shims were manually adjusted to obtain the optimum sensitivity.

2.2. Measurement of radiation damping time constant

The radiation damping time constant (τ_{RD}^{-1}) was determined using inversion recovery of the water magnetization as described by Chen et al. [21] using a standard inversion recovery experiment (180°–τ–90°–acquire). The acquisition time for each transient was 0.682 s over a spectral width of 12,000 Hz. Each FID (free induction decay) was signal averaged over four scans with a recycling delay of 40 s. A total of 107 values of τ was used to range from 0.0001 to 2 s for the inversion recovery. The measurement was repeated in quadruplicate under identical conditions to estimate the experimental error in the measured signal intensity. Time domain data were zero filled once and no apodization was applied prior to complex Fourier transformation. The area under the water resonance was integrated (spectral window of 2500 Hz) and used to determine the radiation damping time constant, as described below.

The time constant of radiation damping (τ_{RD}^{-1}) in SI units is given by [2,19,22]

$$\tau_{RD}^{-1} = 2\pi\eta Q_c \gamma M_0, \tag{1}$$

where η is the filling factor, defined as the ratio of the probe coil volume to the sample volume enclosed within, Q_c is the quality factor of the resonance circuit ($Q_c = \omega L/R$; ω, L, and R are frequency, conductance, and resistance of the resonance circuit, respectively) and γ is the gyromagnetic ratio of the protons. Substituting for M_0, the thermal equilibrium magnetization for spin half nuclei [22], Eq. (1) can be rewritten as

$$\tau_{RD}^{-1} = \frac{\eta Q_c h^2 \gamma^3 N_A B_0}{8\pi kT}, \tag{2}$$

where h is the Planck's constant (6.6262×10^{-34} m^2 kg s^{-1}), N_A is the number of spins per unit volume (typically 6.5×10^{19} protons/1μL of water) [3], B_0 is the strength of the magnetic field in Tesla, k is the Boltzmann constant (1.3806×10^{-23} m^2 kg s^{-2} K^{-1}) and T is the temperature of the sample in K. In general τ_{RD}^{-1} is estimated from the linewidth $\Delta\nu_{1/2}$ (full-width at half-height of a non-Lorentzian lineshape), following a non-selective 90° pulse as [23]

$$\tau_{RD}^{-1} = \frac{\pi \Delta\upsilon_{1/2}}{0.8384}. \tag{3}$$

Eq. (3) provides only a rough estimation of τ_{RD}^{-1} as there are other factors such as relaxation, inhomogeneous broadening, and susceptibility effects that may also contribute to linewidth. Chen et al. [21] have proposed a more precise method to determine τ_{RD}^{-1} which involves fitting experimental data to an analytical description of the recovery of the

magnetization following inversion in systems where the recovery is dominated by radiation damping. During the inversion recovery, under strongly radiation-damping conditions (negligible relaxation effects), τ_{RD}^{-1} is given by

$$\tau_{RD}^{-1}(\tau - \tau_0) = \frac{1}{2}\ln\left(\frac{M_z^{eq} - M_z(\tau)}{M_z^{eq} + M_z(\tau)}\right). \quad (4)$$

Here, τ is the inversion recovery delay and τ_0 is related to the initial azimuthal angle θ_0 of the magnetization following an imperfect inversion pulse from equilibrium (M_z^{eq}) [23]. Linear regression of τ vs. $M_z(\tau)$ was used to estimate τ_{RD}^{-1} (Sigmaplot, Systat Software, Richmond, CA, USA).

3. Results

Fig. 1 shows the plot of the recovery of the Z-magnetization of the water spins in the CapNMR (A), 5 mm (B), and 8 mm (C) probes. Visual inspection of Fig. 1 shows that radiation damping effects are highly active in the CapNMR probe. As expected, the recovery of Z-magnetization due to radiation damping in both the 5 and 8 mm probes is also strong. Table 1 lists the radiation-damping rate constant (τ_{RD}^{-1}), τ_0 and the correlation coefficient of the linear fit of the data to Eq. (4) for each probe. Results in Table 1 clearly show a significant amount of radiation damping in the CapNMR probe (rate constant of 114.1 s^{-1}, which corresponds to a radiation damping time of 8.76 ms). For the 5 and 8 mm probes, the radiation damping rate constants are 108.7 and 554.8 s^{-1}, respectively, with the corresponding radiation damping times of 9.2 and 1.8 ms, respectively. These results compare well with the results of Chen et al. [21], where τ_{RD}^{-1} ranges from 75.8 to 130.0 s^{-1} and τ_0 ranges from 41.2 to 22.4 ms, depending on the amount of H_2O in the sample at the proton resonating frequency of 600 MHz. Radiation damping in the CapNMR probe is much stronger than in the 5 mm probe, but weaker than in the 8 mm probe.

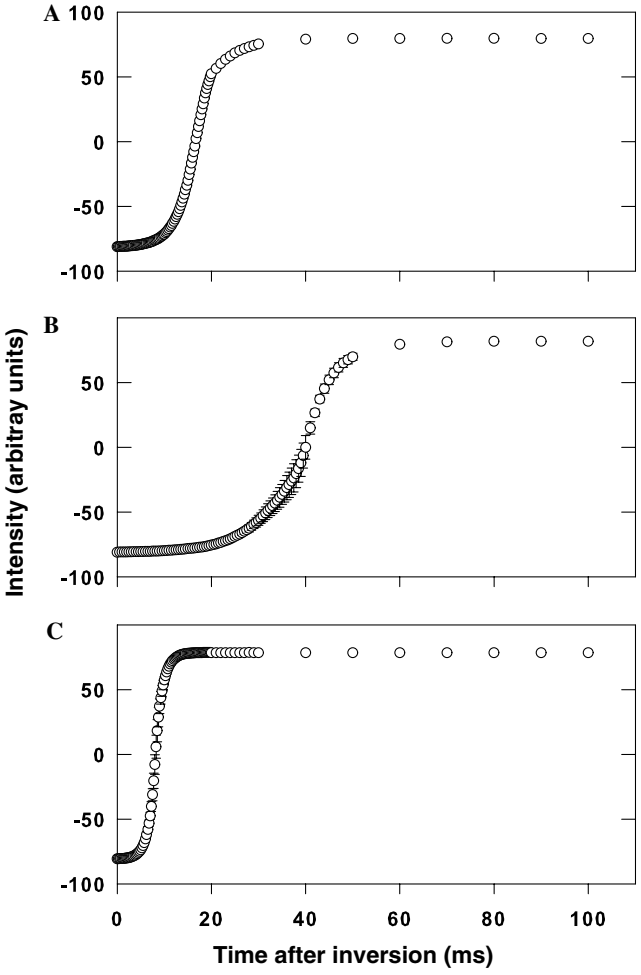

Fig. 1. Plot of the recovery of water magnetization after inversion due to radiation damping in (A) Microcoil NMR probe (CapNMR, 25 μL), (B) standard 5 mm indirect detection probe (5 mm IDPFG, 550 μL), and (C) standard 8 mm triple resonance probe (8 mm TR-PFG, 730 μL). Intensity along the Y-axis the area under the water resonance and the recovery time is along the X-axis. The error bars determine the standard deviation over four consecutive measurements and in (A) the error bars are smaller than the size of the symbols.

Table 1
Radiation damping rate constants in microcoil NMR probe at 600 MHz

NMR Probe	$\tau_{RD}^{-1}(s^{-1})$	τ_0 (ms)	r^2 [d]	Sample (active) volume (μL)
Microcoil[a]	114.10 ± 1.50	1.28 ± 0.03	0.999	25 (5)
5 mm[b]	108.72 ± 5.80	9.09 ± 1.12	0.998	550 (222)
8 mm[c]	554.84 ± 12.34	26.14 ± 4.18	0.965	730 (325)

[a] Microcoil probe (CapNMR)S: Capillary NMR microcoil probe.
[b] Standard 5 mm inverse detection probe.
[c] Standard 8 mm triple resonance probe.
[d] Linear correlation coefficient of the fit to Eq. (4).

Standard errors in the magnetization recoveries in 1 and τ_0 values in Table 1 show that the water magnetization recovers mainly though radiation-damping effects in the CapNMR probe in a much cleaner fashion than in the 5 and 8 mm probes. The latency interval τ_0 is related to the initial azimuthal angle θ_0 of the magnetization following the imperfect inversion pulse, and is given by [23]

$$\frac{\theta_0}{2} = \tan^{-1}(\exp(\tau_0\tau_{RD}^{-1})). \quad (5)$$

Upon using Eq. (5), the azimuthal angles θ_0 for the CapNMR, 5 and 8 mm probes are 26°, 31°, and 44°, respectively. This variation in θ_0 is directly attributable to the external influences (B_0 or RF inhomogeneity) on the metastable state of the inverted magnetization of the water magnetization. Lower values of θ_0 are indicative of less influence from destabilizing factors, such as RF inhomogeneity.

4. Discussion

Standard NMR probes and microcoil NMR probes have few major differences. Most detectors with probe volumes greater that 50 μL described in the literature are based on Helmholtz coils [24,25], which allow easy sample exchange by commercially available NMR glass tubes, as

the coil opening is along the B_0 field. For sample volumes less than 45 μL, a detector is typically designed as a solenoid coil [9,26,27]. The CapNMR probe has a solenoidal detection coil, which must be orthogonal to the B_0 field. As a consequence, the use of conventional NMR sample tubes for sample exchange is not straightforward. Inherently, solenoidal microcoil NMR probes have a higher intrinsic sensitivity [28] than saddle coils (Helmholtz coils) by a factor of 2–3, due to stronger coil-sample coupling. The sensitivity of solenoidal coils is given by [24,25]

$$\frac{B_1}{i} = \frac{\mu_0 n}{d\sqrt{1 + \left(\frac{h}{d}\right)^2}}, \tag{6}$$

where B_1 is the applied radio frequency field, i is the current unit, μ is the permeability in a vacuum, n is the number of turns, d is the diameter of the coil, and h is the length of the coil. Microcoil probes take advantage of decreasing 'd' to increase the sensitivity. The reduction in 'd' subsequently leads to a significant increase in the filling factor (η) of the probe. Typically, recently designed microcoil probes are able to achieve improved values ($\eta \sim 0.64$), while the standard 5 mm probes are able to achieve only $\eta \sim 0.3$ [26]. As the microcoil probes also have good RF homogeneity and the small coils lead to short RF pulses, it is possible to attain an excellent control of the water magnetization in comparison with standard probes.

Based on Eq. (2), radiation damping for the protons at a given probe temperature is directly proportional to: filling factor η, quality factor Q_c and the concentration of the protons in the sample volume. The quantities Q_c and η are often optimized to increase the sensitivity of the NMR probe. Thus, it is natural to expect the radiation damping effects also to increase with an increase in sensitivity. In fact, Guéron and Leroy [3] suggest that τ_{RD}^{-1} can be used as a measure of the absolute sensitivity of the probe, as it is directly proportional to both η and Q_c. For the radiation damping effects in the microcoil probe to be comparable to those in a standard 5 mm probe, the increase in ηQ_c must be of the same order of magnitude as the reduction in the number of water protons.

To determine which factor (η or Q_c) contributes to the radiation damping effects, one can use the measured τ_{RD}^{-1} from Table 1 in Eq. (2) along with other known probe specifications. The ratio of the τ_{RD}^{-1} between the 5 mm and CapNMR probe is 0.95 ($108.72\ s^{-1}/114.1\ s^{-1}$), while the volume ratio is 44.4 (222/5) [26]. Using the filling factor values of 0.3 and 0.64 for the 5 mm and CapNMR probes, respectively, the ratio of the quality factors (Q_c^{5mm}/Q_c^{cap}) of the probes is estimated to be 19.7. This estimate assumes that Eq. (2) provides a valid description of the radiation damping effects in 5 mm (Helmholtz coil) and the CapNMR (capillary) probes. One of the major inferences from this rough estimate is that the effects of radiation damping in the CapNMR probe are due to an increase in the filling factor, η, rather than the quality factor, Q_c.

Extending this observation to probes with cryogenically cooled detector coils that have approximately three times more sensitivity than a standard probe (no cryogenic cooling of the coil), would increase the radiation damping effects by the same factor (3). However, the increased effect will be primarily due to increase in the Q_c, rather than η. This estimation is in confirmation with the preliminary investigation of the radiation damping effects in cryogenically cooled detector coil probe and its impact on heteronuclear experiments [29].

In addition to radiation damping, bulk spin magnetization in NMR experiments is also affected by the dipolar field effects [30,31]. The physics of dipolar field effects, and their similarities to and differences from radiation damping, have recently been presented [32–35]. Radiation damping and dipolar field are proportional to the nuclear spin density and the strength of the external magnetic field. However, unlike radiation damping, dipolar field has a strong dependency on the shape of the sample and the spatial distribution of the nuclear spin magnetization, and more importantly, it is independent of the quality factor (Q_c). A typical 600 μL sample of water in a 5 mm probe and 600 MHz spectrometer produces a dipolar field, resulting in a shift of the NMR signal from the protons on the order of 1 Hz. Considering the shape of the water sample in a microcoil probe to be more spherical, the effect of dipolar fields in the microcoil probe can safely be neglected. These are unique features that enable the isolation of radiation damping effects in the microcoil probe.

In these results, any effects due to the difference in the coil geometry (saddle vs. solenoidal) between the probes, RF field and B_0 inhomogeneity are not considered. According to the detailed work by Augustine and co-workers [20,36], though it is possible to account for inhomogeneous field effects, the effect of coil geometry, if any, is not known.

5. Conclusions

Accurate measurement of the radiation damping time constant in the microcoil (CapNMR) probe, and its comparison with standard 5 and 8 mm probes, clearly suggest that in spite of the significant reduction in the total volume of the water, this probe is significantly affected by radiation damping. The radiation-damping time constant of the CapNMR probe is roughly the same as that of the 5 mm probe, and 1/4th that of the 8 mm probe, at the same spectrometer field strength and sample temperature. Therefore, it is important to optimize the water suppression and water-selective pulses, perhaps more cautiously when using samples with large amounts of H_2O in the microcoil probes. Due to increased RF performance (short pulse widths with good B_0 and B_1 homogeneity), the water selection and control will be more efficient in microcoil probes in comparison with other standard probes, including the cryogenically cooled detector coil probes. These probes provide an excellent experimental avenue for isolating radiation damping

effects in order to explore their role in more complex areas, such as chaotic dynamics [37–39].

Acknowledgments

Thanks to S.P. Mielke for critical reading of the manuscript. The author also thanks Dr. N. Murali (Varian NMR) for discussions and Drs. J. Norcross and T. Peck (Protasis) for information on CapNMR probe parameters. This work was performed under the auspices of the U.S. Department of Energy by the Lawrence Livermore National Laboratory under Contract W-7405-ENG-48.

References

[1] G. Suryan, Nuclear magnetic resonance and the effect of the methods of observation, Curr. Sci. 6 (1949) 203–204.
[2] N. Bloembergen, R.V. Pound, Radiation damping in magnetic resonance experiments, Phys. Rev. 95 (1) (1954) 8–12.
[3] M. Gueron, J.L. Leroy, NMR of water protons—the detection of their nuclear-spin noise, and a simple determination of absolute probe sensitivity based on radiation damping, J. Magn. Res. 85 (1) (1989) 209–215.
[4] M. Gueron, P. Plateau, M. Decorps, Solvent signal suppression in NMR, Prog. Nucl. Mag. Res. Spectrosc. 23 (1991) 135–209.
[5] V. Sklenár, Suppression of radiation damping in multidimensional NMR experiments using magnetic field gradients, J. Magn. Res. Ser. A 114 (1) (1995) 132–135.
[6] J.N. Shoolery, The development of experimental and analytical high resolution NMR, Prog. Nucl. Magn. Reson. Spectrosc. 28 (1) (1995) 37–52.
[7] P. Styles, N.F. Soffe, C.A. Scott, D.A. Crag, F. Row, D.J. White, P.C.J. White, A high-resolution NMR probe in which the coil and preamplifier are cooled with liquid helium, J. Magn. Res. (1969) 60 (3) (1984) 397–404.
[8] T.L. Peck, R.L. Magin, P.C. Lauterbur, Design and analysis of microcoils for NMR microscopy, J. Magn. Res. Ser. B 108 (2) (1995) 114–124.
[9] D.L. Olson, T.L. Peck, A.G. Webb, R.L. Magin, J.V. Sweedler, High-resolution microcoil ^{1}H-NMR for mass-limited, nanoliter-volume samples, Science 270 (1995) 1967–1970.
[10] K.R. Minard, R.A. Wind, Picoliter 1H NMR Spectroscopy, J. Magn. Res. 154 (2) (2002) 336–343.
[11] C.E. Hadden, G.E. Martin, Low-level long-range 1H-15N heteronuclear shift correlation at natural abundance using submicro NMR techniques, J. Nat. Prod. 61 (8) (1998) 969–972.
[12] G.E. Martin, J.E. Guido, R.H. Robins, M.H.M. Sharaf, P.L. Schiff Jr., A.N. Tackie, Submicro inverse-detection gradient NMR: A powerful new way of conducting structure elucidation studies with <0.05 &mgr;mol samples, J. Nat. Prod. 61 (5) (1998) 555–559.
[13] M. Kakuta, D.A. Jayawickrama, A.M. Wolters, A. Manz, J.V. Sweedler, Micromixer-based time-resolved NMR: applications to ubiquitin protein conformation, Anal. Chem. 75 (4) (2003) 956–960.
[14] H. Wensink, F. Benito-Lopez, D.C. Hermes, W. Verboom, H. Gardeniers, D.N. Reinhoudt, A. van den Berg, Measuring reaction kinetics in a lab-on-a-chip by microcoil NMR, Lab on a Chip 5 (3) (2005) 280–284.
[15] W. Peti, J. Norcross, G. Eldridge, M. O'Neil-Johnson, Biomolecular NMR using a microcoil NMR probe–new technique for the chemical shift assignment of aromatic side chains in proteins, J. Am. Chem. Soc. 126 (18) (2004) 5873–5878.
[16] J.C. Rodriguez, P.A. Jennings, G. Melacini, Effect of chemical exchange on radiation damping in aqueous solutions of the osmolyte glycine, J. Am. Chem. Soc. 124 (22) (2002) 6240–6241.
[17] M. Cosman, D.L. Olson, B.E. Hingerty, and P.T.L. NMR Structural Studies of Mass-Limited Modified DNA Using a Protasis/MRM CapNMR Probe. in: The 46th ENC, Experimental Nuclear Magnetic Resonance Conference. 2005. Rhode Island Convention Center, Providence, RI: ENC.
[18] X.A. Mao, C.H. Ye, Understanding radiation damping in a simple way, Concepts Magn. Res. 9 (3) (1997) 173–187.
[19] V.V. Krishnan, Radiation damping: Suryan's line broadening revisited in high resolution solution NMR, Curr. Sci. 74 (12) (1998) 1049–1053.
[20] M.P. Augustine, Transient properties of radiation damping, Prog. Nucl. Magn. Res. Spectrosc. 40 (2) (2002) 111–150.
[21] J.H. Chen, B. Cutting, G. Bodenhausen, Measurement of radiation damping rate constants in nuclear magnetic resonance by inversion recovery and automated compensation of selective pulses, J. Chem. Phys. 112 (15) (2000) 6511–6514.
[22] A. Abragam, The Principles of Nuclear Magnetism, Clarendon Press, Oxford, 1961, p. 73.
[23] X.A. Mao, C.H. Ye, Line shapes of strongly radiation-damped nuclear magnetic resonance signals, J. Chem. Phys. 99 (10) (1993) 7455–7462.
[24] D.I. Hoult, R.E. Richards, The signal-to-noise ratio of the nuclear magnetic resonance experiment, J. Magn. Res. 24 (1) (1976) 71–85.
[25] D.I. Hoult, Sensitivity of the NMR Experiment, in: D.M.G.a.R.K. Harris (Ed.), Encyclopedia of NMR, Wiley, Chichester, 1996, pp. 4256–4266.
[26] M.E. Lacey, R. Subramanian, D.L. Olson, A.G. Webb, J.V. Sweedler, High-resolution NMR spectroscopy of sample volumes from 1 nL to 10 μL, Chem. Rev. 99 (10) (1999) 3133–3152.
[27] R. Subramanian, J.V. Sweedler, A.G. Webb, Rapid two-dimensional inverse detected heteronuclear correlation experiments with <100 nmol samples with solenoidal microcoil NMR probes, J. Am. Chem. Soc. 121 (10) (1999) 2333–2334.
[28] A.G. Webb, S.C. Grant, Signal-to-noise and magnetic susceptibility trade-offs in solenoidal microcoils for NMR, J. Magn. Res. Ser. B 113 (1) (1996) 83–87.
[29] Hallenga, K., M. Tonelli, W.M. Westler, and J.L. Markley. The influence of radiation damping in conventional and cryogenic probes on solvent control in triple resonance experiments and its dependence on sample properties, in: The 46th ENC, Experimental Nuclear Magnetic Resonance Conference, 2005, Rhode Island Convention Center, Providence, RI, ENC.
[30] R. Bowtell, Indirect detection via the dipolar demagnetizing field, J. Magn. Res. (1969) 100 (1) (1992) 1–17.
[31] R. Bowtell, P. Robyr, Structural investigations with the dipolar demagnetizing field in solution NMR, Phys. Rev. Lett. 76 (26) (1996) 4971–4974.
[32] J. Jeener, A. Vlassenbroek, P. Broekaert, Unified derivation of the dipolar field and relaxation terms in the Bloch–Redfield equations of liquid NMR, J. Chem. Phys. 103 (4) (1995) 1309–1332.
[33] A. Vlassenbroek, J. Jeener, P. Broekaert, Radiation damping in high resolution liquid NMR—a simulation study, J. Chem. Phys. 103 (14) (1995) 5886–5897.
[34] A. Vlassenbroek, J. Jeener, P. Broekaert, Macroscopic and microscopic fields in high-resolution liquid NMR, J. Magn. Res. Ser. A 118 (2) (1996) 234–246.
[35] M.H. Levitt, Demagnetization field effects in two-dimensional solution NMR, Concepts Magn. Res. 8 (1996) 77–103.
[36] M.P. Augustine, E.L. Hahn, Radiation damping with inhomogeneous broadening: limitations of the single Bloch vector model, Concepts Magn. Res. 13 (1) (2001) 1–7.
[37] M.P. Augustine, S.D. Bush, E.L. Hahn, Noise triggering of radiation damping from the inverted state, Chem. Phys. Lett. 322 (1–2) (2000) 111–118.
[38] D. Abergel, Chaotic solutions of the feedback driven Bloch equations, Phys. Lett. A 302 (1) (2002) 17–22.
[39] J. Jeener, Dynamical instabilities in liquid nuclear magnetic resonance experiments with large nuclear magnetization, with and without pulsed field gradients, J. Chem. Phys. 116 (19) (2002) 8439–8446.